Solid-liquid equilibria for nitrous oxide+ fluoromethane and triple point measurements for refrigerants

Solid-liquid equilibria for nitrous oxide + fluoromethane and triple point measurements for refrigerants

CRISTIANO DI NICOLA[1], MATTEO MOGLIE[1], GIULIO SANTORI[2],

ROMAN STRYJEK[3], GIOVANNI DI NICOLA[1*]

[1] Dipartimento di Energetica, Università Politecnica delle Marche, Ancona, Italy, 60131

[2] Università degli Studi e-Campus, Novedrate (Co), Italy, 22060

[3] Institute of Physical Chemistry, Polish [3]Academy of Sciences, Warsaw, Poland

Paper presented at the 9th ATPC, Beijing, China, October 19-22, 2010.

ABSTRACT

To evaluate the Solid-Liquid Equilibria (SLE) of alternative refrigerants systems, an experimental set-up was employed. The behaviour of the nitrous oxide + fluoromethane (N_2O + R41) binary system was measured down to temperatures of 126.5 K. The triple point temperature of carbon dioxide, nitrous oxide and of seven of the most widely applied alternative refrigerants, namely fluoromethane (R41), difluoromethane (R32), trifluoromethane (R23), pentafluoroethane (R125), 1,1,1,2-tetrafluoroethane (R134a), 1,1,1-trifluoroethane (R143a) and 1,1-difluoroethane (R152a), were also measured. All triple point data measured revealed a generally good consistency with the literature. The results obtained for the mixtures were corrected by the Rossini method and interpreted by means of the Schröder equation.

Keywords: Fluoromethane; nitrous oxide; refrigerants; solid-liquid equilibria; thermodynamics; triple point.

1 INTRODUTION

Natural gases such as nitrous oxide are considered interesting options as refrigerants for low-temperature applications. In addition, their combination with Hydro-Fluoro-Carbons (HFCs) offers a possible solution as working fluids for

*corresponding author. Email: g.dinicola@univpm.it, tel: +390712204277, fax: +390712204770

cascade cycle units. The main limitation of these binary systems lies on the lowest-temperature limit at which the refrigerant may circulate in the fluid state.

The data on Solid-Liquid Equilibria (SLE) are important in defining the lowest application limit of the systems. In addition, SLE provide theoretical information on the behaviour of studied systems at low temperatures in terms of activity coefficients. However, the SLE for HFCs refrigerants are extremely scarce in the literature.

SLE measurements generally creates difficulties in the visual observation of the disappearance of the last amount of solid phase. For this reason a set-up was specifically built avoiding the need of the visual observation of phase behaviour.

Recently, SLE of several (CO_2 and N_2O) + HFCs binary systems were measured by the same lab [1-5]. In order to describe the behaviour of the binary systems in terms of the Raoult's and Dalton's laws, the *PVTx* of the (CO_2 and N_2O) + R41 binary systems were also recently measured with isochoric and Burnett apparata [6-9]. In this paper, the SLE for the N_2O + R41 binary system was measured down to temperatures of 126.5 K.

Additionally, the triple points of carbon dioxide, nitrous oxide and of seven of the most widely applied alternative refrigerants (R23, R32, R41, R125, R134a, R143a, R152a) were measured.

2 EXPERIMENTAL SET-UP

The experimental setup is shown in figure 1. The apparatus is the same already described in a previous paper [5], where some improvement to the original setup [1-4] was carried out. It comprises a measuring cell and a system for drawing the liquid nitrogen directly from its insulated tank with the aid of compressed air: the carrier fluid circulating in the circuit is thus the refrigerant fluid itself.

The measuring cell (1), with a volume of approximately 47 cm^3, was made out of a stainless steel cylinder with a cover welded to the body. A stirrer (2), consisting of a stainless steel rod having a rounded end with two steel blades welded onto it, was placed in the cell. Two holes were drilled in the cover, and a stainless steel tube was inserted through and welded to the hole on the left for charging the cell with gas, while the hole on the right was used to house the thermometer (3). The function of the stirrer was to prevent any premature stratification of the fluids comprising the various mixtures and to guarantee greater homogeneity during the liquefaction and crystallization of the mixture. The stirrer inside the cell was turned by a magnet, which drives the plate welded onto the lower end of the rod. An absolute pressure transducer (HBM, Mod. P8A) (4) was installed in the charging tube. A mass flow control (5) was installed upstream from the dehumidifier: a needle valve with a shutter was used to adjust the flow rate coming from the dry air supplier (6), as measured by means of the pressure difference read on a pressure gauge alongside it. The airflow was also measured by a rotameter (7).

The operation of the system as a whole can be divided into two separate circuits and consequently two operating modes: a cooling and an heating mode.

The cooling system as a whole is composed by four functional parts: the compressed air circuit that creates a pressure in the liquid nitrogen tank, the thermally-insulated liquid nitrogen tank (8), the hose connecting the tank to the circuit, complete with a faucet, and the copper coil that surrounds and exchanges heat with the cell.

The core element in the whole cooling system is the copper coil surrounding the measuring cell; through its contact surface, the coil removes heat by means of the refrigerant fluid flowing inside it. The copper coil and cell are placed together inside a Dewar flask (9) so as to further isolate them from the outside environment. The system as a whole is suitably covered with neoprene foam for thermal insulation.

When the system is used in the cooling mode, the compressed air (after passing through suitable dehumidifier filters) is delivered to the liquid nitrogen tank. Inside the tank, a PVC hose draws the refrigerant fluid from the bottom, which begins to flow through the circuit as soon as the pressure in the tank, controlled by a manometer (10), is sufficient to overcome the load losses produced by the circuit. When a steady state is reached, the liquid nitrogen flows through the circuit, rapidly cooling all of its surfaces to a very low temperature. The refrigerant fluid passes first through the silicone capillary, then through the copper piping, exchanging heat with the measuring cell by evaporation as it moves through the coil, and finally flows out from the nitrogen outlet (11). In this cooling configuration, the nitrogen valve remains open and the heating circuit valve remains closed.

When the system is operated in the heating mode, the dehumidified compressed air circuit is connected directly to the measuring cell's circuit and, in this case, the air acts as a carrier fluid and warms the cell, which is at a very low temperature by the end of a measuring procedure. In this configuration, the nitrogen inlet valve remains closed. An external copper coil (12) has also been provided: this can be heated by the operator to speed up the warming of the measuring cell.

To monitor the temperatures, the apparatus was equipped with a thermoresistance. The system parameters and the efficiency of the coil immersed in the liquid nitrogen were assessed using thermocouples at specific points on the copper tube. The platinum resistance thermometer used in the apparatus (100 Ω, Minco, Mod. S7929) was calibrated by comparison with a 25 Ω platinum resistance thermometer (Hart Scientific, Mod. 5680 SN1083).

The pressure values were acquired by an absolute pressure transducer (4), which can resist up to $1 \cdot 10^4$ kPa, installed in the charging tube. The test pressure readings were taken with the HBM indicator (model MVD 2405). Data are saved by a powered output on the back of the display proportional to the value displayed, which is connected to one of the terminal board inputs. Thus, the data acquisition software enables us to see the trend of the pressure while

simultaneously and continuously saving the corresponding values. This transducer was calibrated by connecting the transducer to a dead weight gage.

To obtain the temperature and pressure values, a card (PCI NI 435 by National Instruments) for physical data acquisition was installed. The electric terminals of the sensors are not connected directly to the peripheral but communicate via a SH6868 multipolar cable (National Instruments) with a TBX68T terminal board, where the thermocouples, the thermoresistance and the digital pressure transducer are physically connected.

The information sent to the card is processed by a software developed in LabVIEW 6.1. Temperature and pressure readings were acquired approximately every 2.5 s.

3 EXPERIMENTAL PROCEDURE

The charging procedure consisted of the several steps. First, the bottle containing the refrigerant gas (13) was weighed on the electronic balance; then the bottle was connected to the apparatus and to the vacuum pump (14) (Vacuubrand, Mod. RZ2); a vacuum was created inside the measuring cell and the charging tube as recorded on the vacuum pump gauge (Galileo, Mod. OG510); then the fluid was charged by opening the valve on the gas bottle; the temperature of the cell was brought down by a flow of liquid nitrogen so as to insert the whole mass in the cell, leaving as little as possible in the charging tube; a suitable time interval was allowed so that the pressure, being lowered by the temperature reduction, could drop to below atmospheric pressure, then the on/off valve was closed; and the gas bottle was disconnected and weighed again to establish the actual mass charged in the cell.

The coil with liquid nitrogen was wrapped around the measuring cell. Monitoring the time dependence of temperature, a cooling curve was obtained for each sample concentration. While the change of phase occurs, the heat removed by cooling is compensated for by the latent heat of the phase change, showing a change of slope in the temperature trend. The arrest in cooling during solidification allows the melting point of the material to be identified on the time-temperature curve. The melting points can then be plotted versus the composition to give a phase diagram.

4 EXPERIMENTAL UNCERTAINTIES

All the uncertainties were calculated using the law of error propagation. The uncertainty on the mass of fluid charged in the measuring cell was calculated using the law of error propagation. In the calculation of the final global uncertainty on the measurement of the mass charged in the cell, we also took into account both the uncertainty of the estimation of the mass in the tube and the uncertainty deriving from the difference between the two weights.

In the case of a pure component, for the fluids in question we considered the uncertainties due to the electronic balance ($\delta m_w = \pm 0.005$ g), the difference between the two weights ($\delta m_1 = \pm 0.007$ g) and the mass trapped in the tube ($\delta m_{cond} = \pm 10\%\ m_{cond} = \pm 0.005$ g), obtaining a total uncertainty for the mass measurement that was less than ±0.008 g.

The uncertainty δm_{cond} was obtained as follows: $\delta m_{cond} = \pm\ m_{cond}\ [(\delta\rho/\rho)^2+(\delta V/V)^2]^{0.5} = \pm 8.1\%\ m_{cond}$, where $\delta\rho/\rho = 5\%$ (estimate of the density ρ from our experimental *PVT* data) and $\delta V/V = \pm 6.4\%$ (estimate of the volume *V*). So, as an overestimation, it was set as $\delta m_{cond} = \pm 10\%\ m_{cond}$.

When the charge was a binary mixture, in order to follow the procedure described herein, all the above considerations were naturally repeated, so the total uncertainty of the mass of sample mixture was less than ±0.01 g. As a result, the uncertainty in density, calculated with the law of error propagation, was never greater than ±0.05 g/dm^3. The uncertainty in composition measurements was estimated to be always lower than 0.005 in mole fraction.

The uncertainty of the temperature measurements was assessed on the basis of the uncertainty of the reference instrument, the interpolated standard deviation and the uncertainty of the measuring system. The uncertainty of the reference instrument was taken to be 0.0016 K, a value obtained from the calibration certificate for the 25 Ω platinum resistance thermometer issued by the "G. Colonnetti" Metrological Institute in Turin. A standard deviation of ±0.019 K was established from the data obtained by the calibration procedure, evaluated with respect to the difference between the temperature calculated (using the interpolating curve equation) and the temperature measured by the sample sensor. The uncertainty of the measuring system was assessed by observing the temperature oscillations around a constant value, and was taken to be 0.003 K for the calibrated thermoresistance. The total uncertainty for the thermoresistance, using the law of error propagation, was calculated to be less than ±0.023 K. The global uncertainty of the temperature, considering also the accuracy of the detection of the transition temperature and contribution of the Rossini method, was estimated to be lower than ± 1 K.

Since the measured vapour-pressure data were not accurately measured at very low temperatures within the declared precision of the used instrument (the pressure values were acquired by an absolute pressure transducer and the global uncertainty of the pressure measurements was estimated to be less than 3 kPa), the vapour-pressure data were not reported in the present paper.

5 EXPERIMENTAL RESULTS

5.1 Chemicals

Nitrous oxide was supplied by Sol Spa. Its purity was checked by gas chromatography, using a thermal conductivity detector, and was found to be 99.99% basing all estimations on an area response. R41 was supplied by Lancaster Inc.; its purity was found to be 99.9% on an area response.

5.2 Pure fluids

Different tests were conducted for all the tested pure fluids, using different configurations (with the stirrer on or off). The values obtained with the stirrer on reveal a lesser discrepancy vis-à-vis those reported in the literature, bearing witness to the fact that the homogenizing effect of the stirrer on the temperature of the fluid in the measuring cell has a beneficial influence on the reliability of the test results. Table 1 summarizes the averaged temperatures recorded at the triple point for the carbon dioxide, nitrous oxide, R23, R32, R41, R125, R134a, R143a, R152a and the available literature data for these fluids. Each triple point measurement was obtained in different experiments, and different runs were repeated for each pure fluid.

For carbon dioxide, the tests conducted revealed a wide metastable phase [1], and a very good agreement with the literature source [10]. About the binary system's constituents, for nitrous oxide, an acquisition run was shown in figure 2. From this figure it is evident a subcooling of few degrees due to the metastable state. Triple-point measurements (T_{tp}=182.0 K) showed a generally good agreement with the literatures sources (T_{tp}=182.34 K) [11-12]. For R41, the metastable phase was not observed during the measurements, and better results were achieved with the system operating in the heating mode. In this way, a change of slope was evident in the temperature-time diagram during the heating, as witnessed by figure 3. The triple point measurement (T_{tp}=129.8 K) revealed a very good consistency with the literature value (T_{tp}=129.82 K) [13].

Also for the other refrigerants for which the triple point temperature was measured (R23, R32, R125, R134a, R143a and R152a), the metastable state was not observed during the measurements. However, a change of slope was always evident in the temperature-time diagram during the heating mode. From the results summarized in Table 1, a generally good agreement with all the literature sources is evident [14-18].

5.3 Results for mixtures

Regarding the studied mixtures, no literature data on the SLE of the analyzed binary system are available in the open literature. Measurements were taken using different concentrations of the two components, obtaining a satisfactory number of points, which were then recorded on a concentration/temperature graph (T-x).

Conducting several tests on the same sample, we noted that we obtained more reliable results by switching off the stirrer at least about 20-40 K (values suggested by experience) before reaching the triple point temperature. This was

probably due to the turning of the stirrer, that helps to keep the mixture's components well mixed and the homogeneity of temperature inside the cell, but once near-freezing temperatures have been reached, it probably interferes with the solidification of the mixture, fragmenting the solid crystals when they began to form.

In addition, conducting several tests on different sample compositions, better results were generally achieved when the apparatus was used in the cooling mode; at very high R41 concentrations, results obtained with the apparatus in the heating mode were found to be more reliable. In figures 4 and 5, two examples of the acquisition curves for the binary system were reported, with measurements obtained both adopting the cooling mode (figure 4) and the heating mode (figure 5). When possible, however, data were collected with both configurations for the same concentrations and results were mutually consistent, with deviations always well within 1 K. This value could be considered the reproducibility limit of our experimental measurements.

This is confirmed by figure 6, where the *T*-*x* measurements for the system considered are reported. The results were also summarized in Table 2. From the *T*-*x* data it is evident that the system forms eutectics ($x_1 = 0.16$ at $T = 127$ K).

5.4 Rossini method corrections

The results of the temperature data acquisitions were corrected using the Rossini method [19] because a constant cooling rate is not indispensable and was not guaranteed by our experimental method. The entity of the corrections takes into account the fact that the fluid is still in a liquid state during the metastable state (supercooling) that precedes proper solidification. In this phase, the temperature is distinctly lower than the one characterizing the instant when crystallization begins, its amplitude depending mainly on the rate at which the temperature is lowered. The resulting corrections were nonetheless always very limited, of the order of a few tenths of a Kelvin in the majority of cases, and always well below 1 K.

6 INTERPRETATION OF THE RESULTS

When an organic system forms eutectic, the course of the *liquidus* is well described by the Schröder equation [20]. The SLE depend both on the crystals formed in solution and on the properties of the liquid phase. VLE derived from our previous isochoric measurements for the binary system under study witnessed that the system showed an almost ideal behavior in terms of the Raoult's law [9]. The exact course of the *liquidus* for mixtures showing a small deviation from Raoult's law depends mainly on the enthalpy of fusion of the solute (N_2O in our case).

As both systems formed eutectics, the solubility of the solid solute in the solvent (here, R41) can be described by the Schröder equation; which disregarding any difference between the heat capacity of the subcooled liquid solute and solid solute takes the following form:

$$\ln \gamma_2 x_2 = \frac{\Delta h_m}{RT}(1 - \frac{T}{T_m}) \quad (1)$$

where the subscript 2 denotes the solute and the subscript m denotes property at melting point. Since the system showed an almost ideal behavior in terms of the Raoult's law, it is possible to assume as a first approximation that the solute's activity coefficient, γ_2=1, so we can write:

$$\ln x_2 = \frac{\Delta h_m}{RT}(1 - \frac{T}{T_m}) \quad (2)$$

This simplification leads to the consideration that the solubility of the solid solute is independent of the solvent as far as the assumptions hold. The enthalpies at melting point (Δh_m) were assumed to be 6540 J·mol^{-1} [21] and 4590 J·mol^{-1} [22] for N_2O and R41, respectively.

The course of the liquidus calculated with the Schröder equation is included in figure 6. The system well followed the Schröder equation.

7 CONCLUSION

Solid-liquid equilibria of nitrous oxide + fluoromethane (N_2O + R41) was measured down to temperatures of 126.5 K. The binary system is potentially suitable working fluids in low-temperature refrigeration applications, as cascade cycles. The triple point temperature of carbon dioxide, nitrous oxide, fluoromethane, difluoromethane, trifluoromethane, pentafluoroethane, 1,1,1,2-tetrafluoroethane, 1,1,1-trifluoroethane and 1,1-difluoroethane were also measured revealing a good consistency with the literature.

The measurements were performed both in the cooling and in the heating mode. The two configurations showed mutually consistent results.

The N_2O + R41 system showed the presence of an eutectic at temperatures very close to R41 triple point temperature (about x_1 = 0.16 at T = 127 K) and a general agreement with the Schröder equation was evident.

NOMENCLATURE

P	pressure	[bar]
T	temperature	[K]
x	bulk composition	(mole fraction)
R	gas constant	[J·K^{-1}·mol^{-1}]
h	enthalpy	[J·mol^{-1}]
Ω	ohm	

Δ	variation
γ	activity coefficient
tp	triple point
m	melting point
2	solute
SLE	solid-liquid equilibrium
PVTx	pressure-volume-temperature-composition
VLE	vapor-liquid equilibrium
HFCs	hydrofluorocarbons
CO_2	carbon dioxide
N_2O	nitrous oxide
R23	trifluoromethane
R32	difluoromethane
R41	fluoromethane
R125	pentafluoroethane
R134a	1,1,1,2-tetrafluoroethane
R143a	1,1,1-trifluoroethane
R152a	1,1-difluoroethane

REFERENCES

[1] Di Nicola G., Giuliani G., Polonara F. and Stryjek R. *J Chem Eng Data* **51**(2006) 2209.

[2] Di Nicola G., Giuliani G., Polonara F. and Stryjek R. *Fluid Phase Equilib.* **256**(2007) 86.

[3] Di Nicola G., Santori G. and Stryjek R. *J Chem Eng Data* **53**(2008) 1980.

[4] Di Nicola G., Giuliani G., Polonara F., Santori G. and Stryjek R. *Int J Thermophys.* **31**(2010) 1880.

[5] Di Nicola G., Moglie M., Santori G. and Stryjek R. *Int J Thermophys.* **30**(2009) 1155.

[6] Di Nicola G., Giuliani G., Polonara F. and Stryjek R. *Fluid Phase Equilib.* **225**(2004) 69.

[7] D'Amore A., Di Nicola G., Polonara F. and Stryjek R. *J Chem Eng Data*. **48**(2003) 440.

[8] Di Nicola G., Polonara F., Ricci R. and Stryjek R. *J Chem Eng Data.* **50**(2005) 312.

[9] Di Nicola G,, Giuliani G,, Polonara F, and Stryjek R. *Fluid Phase Equilib.* **230**(2005) 81.

[10] Angus S,, Armstrong B, and de Reuck K, M. International Thermodynamic Tables of the Fluid State - 3 Carbon Dioxide, New York: Pergamon; 1976.

[11] Calado J. C. G., Rebelo L. P. N., Streett W. B. and Zollweg J. A. *J Chem Thermodyn*. **18**(1986) 931.

[12] Fonseca I. M. A. and Lobo L. Q. *Fluid Phase Equilib.* **47**(1989) 249.

[13] Holcomb C. D., Magee J. W., Scott J. L., Outcalt S. L. and Haynes W.M. NIST Technical Note1397. Gaithersburg: NIST; 1997.

[14] Magee J. W. and Duarte-Garza H. A. *Int J Thermophys*. **21**(2000) 1351.

[15] Lüddecke T. O. and Magee J. W. *Int J Thermophys.* **17**(1996) 823.

[16] Tillner-Roth R., Baehr H. D. *J Phys Chem Ref Data*. **23**(1994) 657.

[17] Magee J. W. *Int J Thermophys.* **19**(1998) 1397.

[18] Blanke W. and Weiss R. *Fluid Phase Equilib*. **80**(1992) 179.

[19] Mair B. J., Glasgow J. A. R. and Rossini F. D. *J Res Nat Bur Standards*. **26** (1941) 591.

[20] Schröder I. *Z Phys Chem*. **11**(1893) 449.

[21] Lide D. R. and Kehiaian H. V. CRC Handbook of Thermophysical and Thermochemical Data; Boca Raton: CRC Press; 1994.

[22] Rowley R. L, Wilding W. V., Oscarson J. L., Yang Y. and Giles N. F. DIPPR Data Compilation of Pure Chemical Properties, Design Institute for Physical Properties. New York: AIChE; 2010.

TABLE 1. Triple Point Temperature Measurements for CO_2, N_2O, R23, R32, R41, R125, R134a, R143a and R152a.

Fluid	*Sample purity*	T_{lit}	*Sources*	T_p
CO_2	99.99 %	216.58	[10]	216.6
N_2O	99.99 %	182.34	[11-12]	182.0
R23	99.6 %	118.02	[13]	117.7
R32	99.98 %	136.34	[14]	137.1
R41	99.9 %	129.82	[12]	129.8
R125	99.96 %	172.52	[14]	173.0
R134a	99.98 %	169.85	[15]	169.7
R143a	99.9 %	161.34	[16]	161.4
R152a	99.94 %	154.30	[16-17]	154.3

TABLE 2. *T-x* Measurements for the N_2O + R41.

$N_2O(1)$ + R41 (2)	
x_1	T / K
0.000	129.77
0.035	131.05
0.036	129.15
0.052	130.02
0.090	128.55
0.099	128.35
0.157	128.65
0.249	137.64
0.249	137.62
0.298	142.05
0.298	141.85
0.345	145.04
0.397	150.95
0.397	151.55
0.452	154.35
0.498	156.84
0.633	164.75
0.662	166.85
0.696	167.16
0.790	174.15
0.831	174.18
0.831	174.15
0.866	176.15
0.889	175.35
0.923	178.92
0.923	179.00
0.938	178.05
1.000	181.99

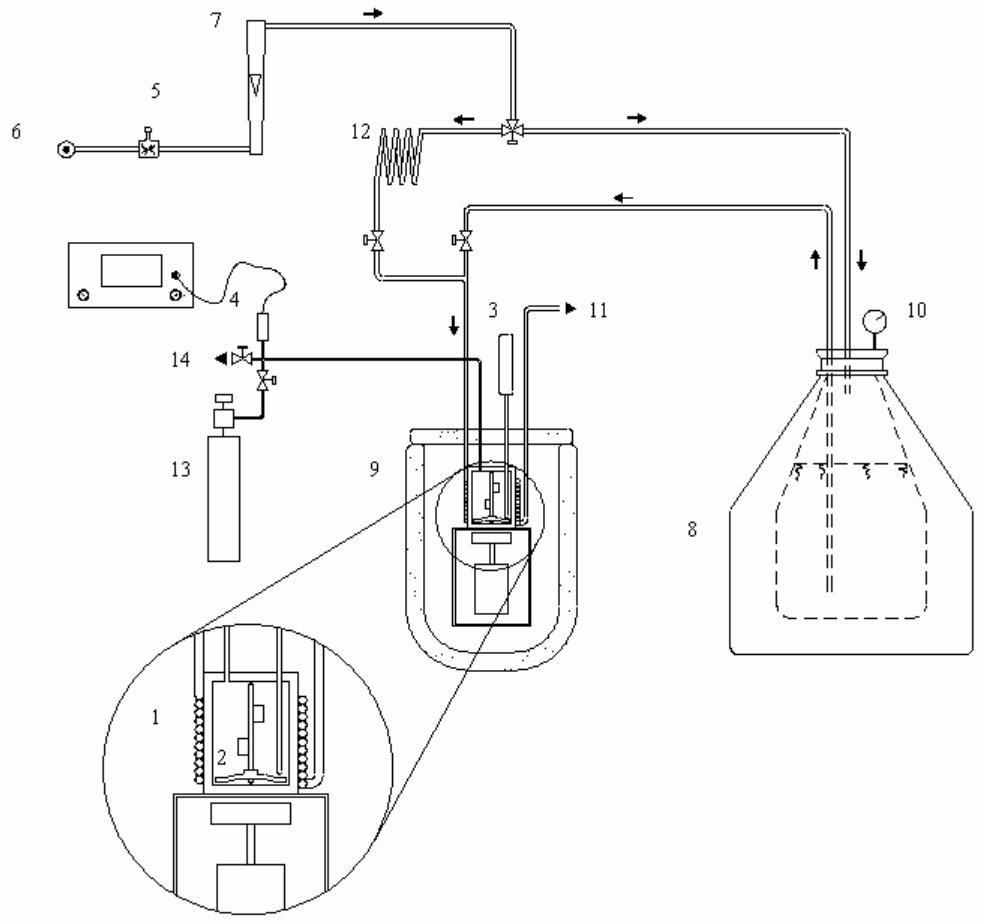

(1) Measuring cell; (2) Stirrer; (3) Platinum resistance thermometer; (4) Pressure transducer; (5) Mass flow controller; (6) Dry air supplier; (7) Rotameter;(8) Liquid nitrogen tank; (9) Dewar containing the measurement cell; (10) Liquid nitrogen dewar manometer; (11) Nitrogen outlet; (12) External heating coil; (13) Charging bottle; (14) Vacuum pump system.

FIGURE 1
Experimental setup.

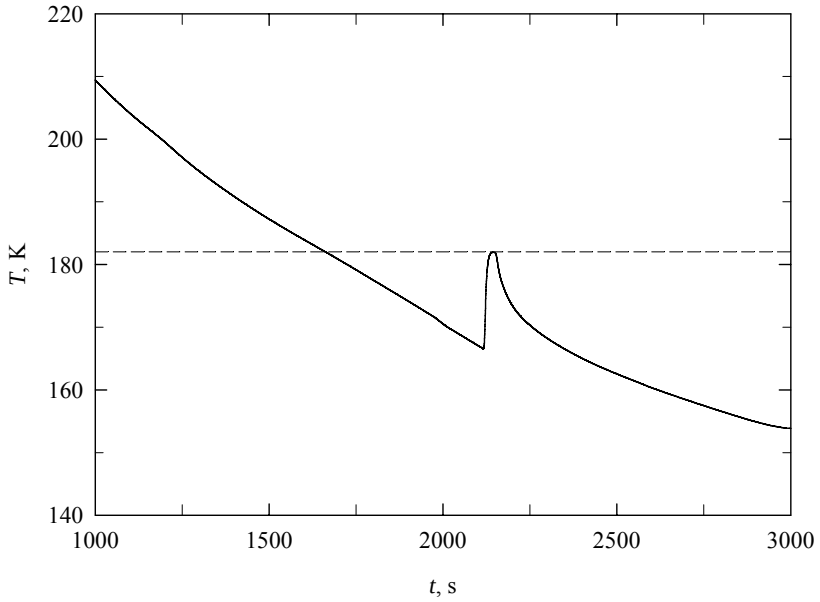

FIGURE 2
Acquisition of N_2O triple point temperature measurements.

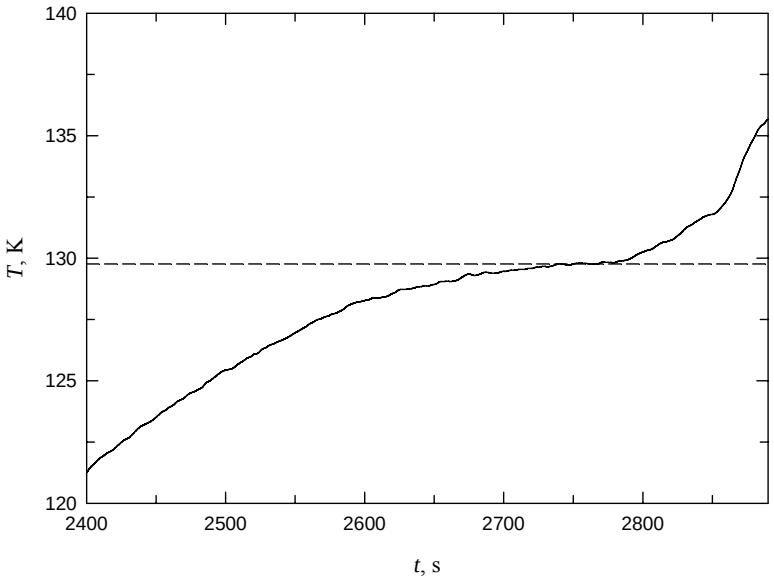

FIGURE 3
Acquisition of R41 triple point temperature measurements.

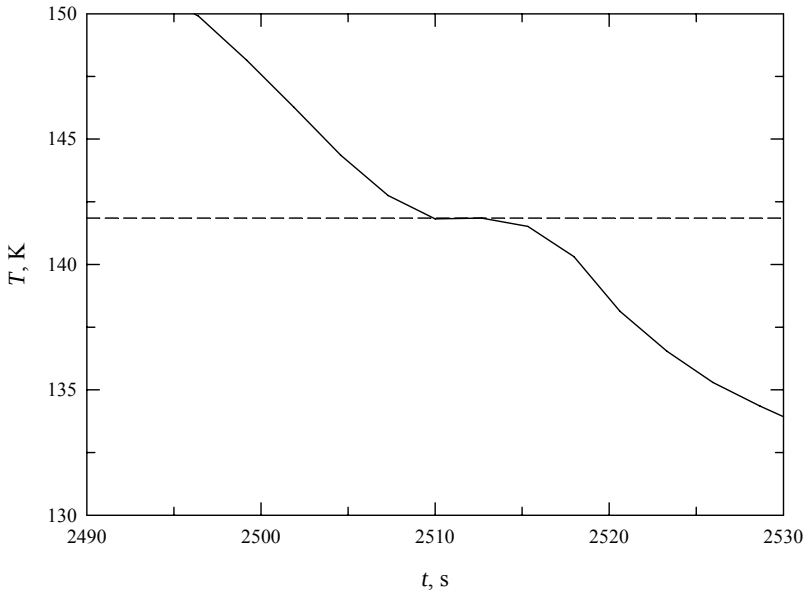

FIGURE 4
Example of acquisition for the N_2O + R41 binary system at mole fraction of x_1=0.298.

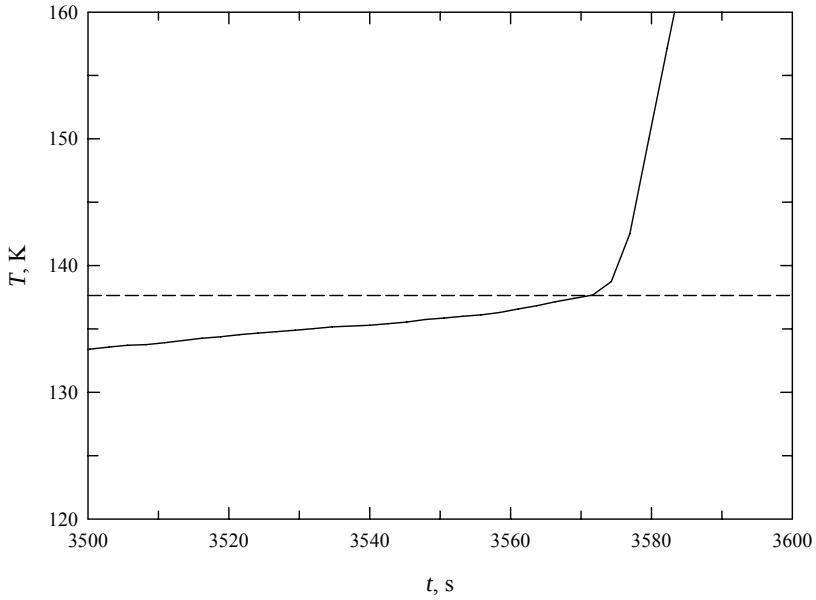

FIGURE 5
Example of acquisition for the N_2O + R41 binary system at mole fraction of x_1=0.249.

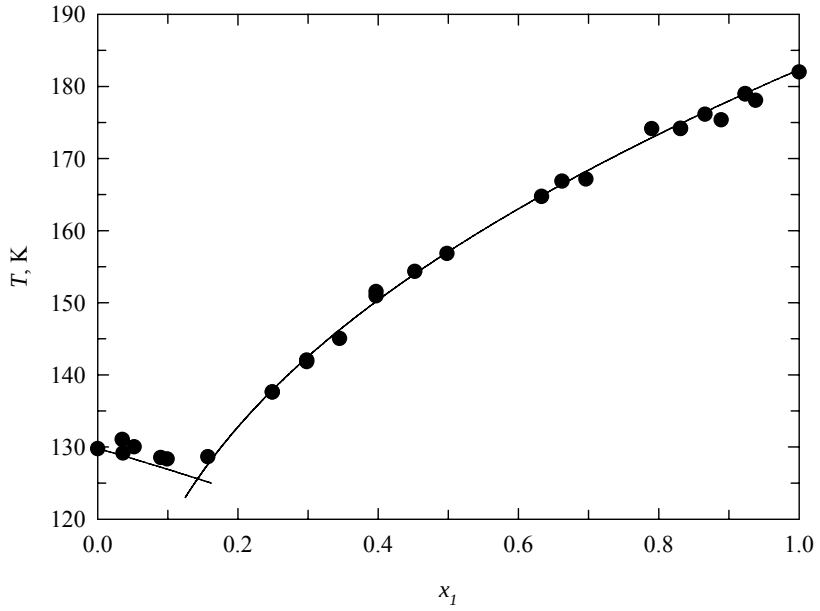

FIGURE 6
SLE for the N_2O + R41 system. Black symbols denote the experimental points, while the lines denote the Schröder equation.